

Strain induced extrinsic magnetocaloric effects in $\text{La}_{0.67}\text{Sr}_{0.33}\text{MnO}_3$ thin films, controlled by magnetic field

S. K. Giri¹, J. L. MacManus-Driscoll^{1*}, W. Li¹, R. Wu¹, T. K. Nath² and T. S. Maity^{1,*}

¹Department of Materials Science & Metallurgy, University of Cambridge, 27 Charles Babbage Road, Cambridge CB3 0FS, United Kingdom

²Department of Physics, Indian Institute of Technology Kharagpur, 721302, India
Corresponding authors: jld35@cam.ac.uk; tsm38@cam.ac.uk

Abstract

The magnetic control of strain-induced giant caloric properties of epitaxial $\text{La}_{0.67}\text{Sr}_{0.33}\text{MnO}_3$ (LSMO) thin films grown on (001) BaTiO_3 (BTO) single crystal substrates is investigated. Arising from the crystallographic structural transformation of the BTO substrate during its 3-phase transitions, there is a drastic change of 3-dimensional film-lattice strain, which affects the local magnetic anisotropy of the LSMO at the interface and changes the entropy of the film. The thermal hysteresis observed in temperature dependent resistivity measurement can be manipulated by applying a magnetic field. Detailed transport and magnetic studies in different crystal orientations reveal the origin of such field-dependent magnetocaloric properties induced by the different phase transitions of the BTO substrate. Finally, a large entropy change of $1.03\text{-}1.95 \text{ J.Kg}^{-1}.\text{K}^{-1}.\text{T}^{-1}$ was obtained at the monoclinic-tetragonal (M-T) transition at 283 K which compares to $<1 \text{ J.Kg}^{-1}.\text{K}^{-1}.\text{T}^{-1}$ for previously reported films.

1. Introduction

Caloric materials are used for a wide range of applications such as refrigeration, air-cooling, etc. In recent years due to the advancement of Internet of Things (IoT), various nanostructured multicaloric materials which show thermal changes driven by more than one type of external parameter are being investigated for a wide range of applications like solid-state refrigeration devices, caloric-sensors, and energy harvesting. [1,2] Ferroic materials with first-order phase transitions show large caloric effects due to the required large latent heat during temperature-dependent phase transitions. However, the number of such materials is very limited. [2, 3] Recently in colossal magnetoresistive (CMR) systems, the giant magnetocaloric effect has been observed where strain is induced by structural transitions resulting in adiabatic thermal processes. [4-6] Significant changes in caloric properties can be manipulated in these multicaloric materials by more than one type of external field. [7]

$\text{La}_{0.7}\text{Sr}_{0.3}\text{MnO}_3$ (LSMO)/ BaTiO_3 (BTO) is one of the most interesting multicaloric systems, which has been studied by various groups not only for its potential multicaloric device applications but also for the fundamental understanding. [2, 7, 8] In this system, ferroelectric BTO undergoes three successive phase transitions as a function of temperature: the rhombohedral to monoclinic (R-M) at 183 K, the monoclinic to tetragonal (M-T) at 283 K, and the tetragonal to cubic (T-C) at 393 K. When half metallic LSMO is grown epitaxially on BTO, the interfacial strain induced by the lattice mismatch and variation in crystal symmetry of BTO around its three first order structural phase transitions strongly modifies the magnetic and transport properties of the LSMO. [9-12] During the phase transition in BTO, thermal hysteresis is observed in the temperature dependent resistive measurements of LSMO during heating and cooling cycles. Such effect is observed in

various magneto-caloric materials deposited on BTO originated due to magnetic domain rotations, driven by the change in strain-induced local magnetic-anisotropy axes. [7, 13-15]

In this report, we studied the effect of magnetic field on the substrate-strain-induced magnetocaloric properties of epitaxial 500 Å LSMO thin films grown on BTO, as well on the tuneability of the properties. We find that the thermal hysteresis observed in resistivity measurements at zero bias field for M-T and T-C phase transitions is suppressed, and even vanishes in the presence of an external magnetic field. We find this to originate from a change in the substrate-induced magnetic domain growth in the LSMO. This suppression of domain growth arises from the strain-induced local magnetic anisotropy modification of LSMO in the different layers. To investigate the origin of the magnetic field dependent caloric effect, both the transport and magnetic properties of the LSMO-BTO film are investigated in different orientations of the magnetic field. The observed strain dependent magnetocaloric effect (MCE) offers potential applications for caloric devices such as solid-state refrigeration, caloric sensors, and caloric energy harvesters.

2. Experimental details

Epitaxial LSMO film with a thickness of 500 Å was grown on (001) BTO substrate by 90° off-axis RF-magnetron sputtering. An rf (13.56 MHz) power of 100 W was used. The process was carried out in a flowing gas mixture of argon with oxygen in the 12:8 volumetric ratios with 200 mTorr total pressure. The growth temperature for the substrate was optimized at 750° C. After deposition, the films were cooled under ambient oxygen of 300 Torr. Detailed structural characterization was carried out by at room temperature using a four circle x-ray diffractometer with Cu K_α radiation, high-resolution transmission electron microscopy (HRTEM) and atomic force microscopy (AFM). Temperature-dependent magnetoresistance (MR) measurements were

carried out in a Quantum Design Physical Property Measurement System (PPMS) and the temperature-dependent magnetic measurements were done in a Quantum Design SQUID Magnetic Property Measurement System (MPMS). For the resistivity measurement, the current was applied along the plane of the film while the magnetic field was applied in three different configurations: parallel to the current ($H \parallel J$), perpendicular to the current ($H \perp J$) and out of plane ($H \odot J$). The temperature-dependent MR measurements were carried out for several temperatures at 300 K, 260 K, 200 K, 165 K, and 4.2 K in all 3 magnetic field configurations across the three phase-transition temperatures of BTO. Magnetic measurements were carried-along the in-plane and out-of-plane directions and across the R-M and M-T phase transitions. A small ramp rate of the magnetic field, i.e., 10 Oe per minute was used for very slow magnetic field scan in the SQUID to consider all the magnetization process as quasi-equilibrium and isothermal. Further initial magnetization hysteresis curves were measured for different temperatures to investigate the effect of the magnetic field on the magnetocaloric properties of the film. The sample was properly demagnetized before each magnetic measurement.

3. Results and discussion

The in-plane, out-of-plane lattice parameters and the associated three-dimensional (3D) strain states in the films were determined by normal X-ray diffraction at room temperature [Figure 1]. The bulk LSMO target has a pseudocubic perovskite structure with lattice parameters $a^p = 3.884$ Å. The tilting of MnO_6 octahedral in LSMO results in a rhombohedral structure with relation $a^{Rhom} = \sqrt{2}a^p$ and $\alpha = 60^\circ$. The pseudocubic lattice parameters are rotated 45° from the rhombohedral lattice parameters (a^{Rhom}). In this paper we have described the Miller indices of the LSMO planes based on pseudocubic perovskite unit cell structure. At film deposition temperature the substrate

is in cubic phase. At room temperature in tetragonal phase, the a-axis and c-axis lattice parameters of BTO substrate are 3.997 Å and 4.037 Å ($c/a = 1.01$), respectively.

The out-of-plane pseudocubic lattice spacing (d_{001}) of the film is obtained to be (3.841 ± 0.005) Å. The in-plane lattice spacing of the film from grazing incidence x-ray diffraction (GID) is found to be $3.942 (\pm 0.006)$ Å. This indicates that the LSMO film has an in-plane biaxial tensile strain with $\varepsilon_{xx} = \varepsilon_{yy} = +1.5\%$ and out-of-plane uniaxial compression of $\varepsilon_{zz} = -1.1\%$. We also found that the volume of LSMO is expanded by 1.8%. Well known, the strain created by the lattice mismatch between film and substrate -in epitaxial manganite film can be decomposed into bulk strain,

$$\varepsilon_B = \varepsilon_{xx} + \varepsilon_{yy} + \varepsilon_{zz} \quad (1)$$

and a volume preserving Jahn-Teller strain,

$$\varepsilon_{JT} = \sqrt{1/6} (2\varepsilon_{zz} - \varepsilon_{xx} - \varepsilon_{yy}) \quad (2)$$

The bulk strain and Jahn-Teller strain is calculated to be $\varepsilon_B = 1.9\%$ and $\varepsilon_{JT} = -2.1\%$. This implies that the LSMO film is not fully strained (partially strain relaxed) to the BTO substrate because of a large biaxial tensile stress caused by the lattice mismatch (2.9%). [9]

Temperature-dependent electrical resistivity (ρ) measurements of LSMO films were studied in the temperature range 4.2 - 415 K in both warming up and cooling down cycles. Figure 2 (a) shows the low temperature resistivity measurements in the temperature range 4.2 - 350 K with both zero bias field and 50 kOe bias fields. For a zero bias field two jumps in electrical resistivity of LSMO/BTO film at 185 K and 280 K temperatures were observed, at the R-M and M-T phase transitions of the BTO substrate, respectively. A further jump at 400 K in the high temperature measurement from 305 K to 415 K was also observed which is associated with T-C phase transition of BTO [Figure 2 (b)]. Interestingly if a bias field of 5T is applied, the two jumps

at the M-T transition at 280K and the T-C transition at 400 K vanish from the temperature-dependent resistivity measurement, but the jump at 185K for the R-M transition remains which is conspicuous. The inset figures show significant thermal hysteresis in the resistivity measurements for heating and cooling cycles where the transition temperatures for the resistivity jumps are enhanced by $\Delta T = + 9.5$ K around 180.5 K, $\Delta T = + 5$ K around 277K, and $\Delta T = + 5$ K around 400 K in the warming-up cycle compared to those in the cooling cycle. These temperatures are very close to the phase transition temperatures of the BTO substrate.

In the magnetization vs. temperature measurement for cooling and warming cycles, a similar thermal hysteresis was observed at the R-M and M-T transitions where the loop is much more prominent for the in-plane magnetization compared to the out-of-plane magnetization [Figure 3(a)]. In the presence of a high magnetic field (50 kOe), the thermal hysteresis vanishes [Figure 3(b)]. To understand the effect of strain on the magnetic properties of the LSMO film during phase transitions, magnetic hysteresis loops were measured for both in-plane and out of plane direction for just above and below the phase transition temperatures [Figure 3 (c & d)]. The magnetic properties of LSMO changes drastically due to the phase transition of BTO. It was observed that the out-of-plane magnetization remains nearly unchanged for both the transitions at just below and above the transition temperature, and is dominated by the shape anisotropy of the film. The in-plane remanence (M_R) and saturation magnetization (M_S) increases (ΔM_S) with decrease of temperature for both transitions but the out-of-plane remanence and saturation magnetization remains unchanged. As BTO is nonmagnetic the change in M_R and M_S can originate only from LSMO. This indicates modification of the crystal structure in BTO due to the phase transition which in turn modifies the magnetization of the interfacial LSMO. As a result, in the interfacial LSMO the local magnetization increases due to the inhomogeneous strain and the

relative change in the entropy of the film. [16] This change in entropy is much higher at the R-M transition compared to the M-T transition since both the resistive and magnetic thermal hysteresis loops are bigger at the R-M transition. However, in T phase the magnetic anisotropy of the film became higher in the [100] direction compared to the other phases. As the energy product (BH_{\max}) in the [100] direction is low for the T phase, the thermal hysteresis readily vanishes at the M-T transition upon application of an external field. In other words, the energy required for M-T phase transition obtained from the applied field is less, and so no thermal hysteresis is observed. It is very likely that the octahedral rotations of MnO_6 in the interfacial LSMO layers during the phase transition are influenced by the induced strain [7, 9] and results in magnetic field dependent anisotropy.

The observation of sharp jumps in resistivity near the substrate structural transformation is due to the presence of the biaxial strain, E_{bi} , induced by the lattice mismatch between the film and substrate. [9, 17] In the resistivity vs. temperature measurements with a 50kOe magnetic bias field, it is clearly observed that not only do the resistivity jumps at higher temperatures (277 K and 400 K) completely disappear but also the jump at a lower temperature (180.5 K) is reduced in magnitude. Similarly, upon application of the magnetic field, the thermal hysteresis in resistivity vanishes at a higher transition temperature. However, a smaller hysteresis is still observed at the lower temperature phase transition at 180.5 K for the R-M transition. This magnetically-driven transition occurs due to the difference in the magnetostrictive strain at the LSMO-BTO interface. The strain is much higher near the interface and it decreases as the distance from interface increases. As a result, different magnetization states can coexist in the LSMO film depending on the localized strain and modifies the orientation of the local magnetic-anisotropy axes and the corresponding change in entropy. Additionally, this relative magnitude of the modified biaxial

strain at the LSMO-BTO interface is different in the different phases of BTO since the structural transitions of BTO are different. This results in different local magnetic anisotropies for different phase transitions. As shown in Table 1, the change in E_{bi} is -0.23%, 0.25% and 0.45% at $T = 180.5$ K (R-M transition), $T = 277$ K (M-T transition) and $T = 393$ K (T-C transition) respectively. Since the strain at the R-M transition is nearly double that at the other two transitions the strain induced magnetic anisotropy change is also higher, and thus so is the change in entropy.

To understand the effect of magnetic field on the thermal hysteresis of the resistivity measurements, the field-dependent resistivity, i.e. magneto-resistivity (MR) measurements were done at 5 different temperatures: 4.2 K, 165 K, 200 K, 260 K and 300 K across the phase transitions of BTO. The magnetic field (H) was applied in three different directions: parallel (\parallel), perpendicular (\perp) and out-of-plane (\odot) with respect to the current (J) [Figure 4 (a)]. The observed negative MR effect which increases with field arises from the suppression of spin fluctuations with the application of a magnetic field [Figure 4 (a)]. The rate of this increase is much higher above the R-M transition temperature [Figure 4 (b)]. At low field, an intersecting difference is observed for these three configurations [Figure 5]. A flat plateau region with negligible MR is observed in the low field regime in the out-of-plane configuration ($H \odot J$). The flat plateau comes from the decreasing demagnetizing field, $H_{d\text{mag}} = NM_S$ (N = demagnetizing factor), and competes with the external magnetic field and tends to keep the magnetization along in-plane direction. This result implies that conduction electrons cannot "feel" the change because of the demagnetizing field and thus no MR effect is observed in the low field regime. Besides, the flat plateau region gets contracted with an increase of temperature from 4.2 K to 300 K [Figure 5(a)]. Further, we observe a positive non-linear MR in the low field region in the case of the $H \perp J$ configuration, which crosses over to negative MR at relatively higher fields [Figure 5(b)]. This low field positive MR

is observed due to the competition between transverse and longitudinal domain formation at the $H \perp J$ configuration where the field and current are in-plane but perpendicular to each other. Interestingly, such non-linearity is not observed at very low (4.2 K) or high (400 K) temperature which could be related to the BTO phase and its strain which effect the transverse and longitudinal domain formation differently.

The effect of magnetic field on the temperature dependent resistivity is investigated in all three directions where the data is extracted from field dependent MR measurement for different temperatures. At low fields, the temperature-dependent resistivity behaves differently in the three directions due to the evolution of the strain-induced local magnetic anisotropy in the different layers of LSMO [Figure 6 (a-c)]. In the $H \parallel J$ configuration, the resistivity linearly increases with a temperature below the R-M phase transition. Above that, it monotonically increases in the negative direction. In the $H \perp J$ configuration, a small change in magnetic field-dependent resistivity in the positive direction is observed at the R-M phase transition. As the temperature increases above the R-M transition, a drastic change in resistivity in the negative direction is observed as a function of applied field. No significant change is observed in $H \circ J$ configuration. This explains that, for R-M phase transition, the effect of strain is much higher which reduce the degrees of freedom of the transverse and longitudinal domains and thus reduce the effect of magnetic field. Hence, the magnetic field cannot suppress the magnetic entropy due to the large strain-induced local magnetic anisotropy, and the thermal hysteresis is still observed at this transition even with applying a 50 kOe magnetic field.

On the other hand, the strain at the M-T and T-C transitions is lower. This results in the coexistence of high-strained and low-strained magnetic domains that allow both transverse and anti-parallel domains to minimize the entropy of the system in the presence of a magnetic field.

Hence, the thermal hysteresis is suppressed. This means that the thermal energy required for the R-M phase transition is much higher than the other transitions. A much higher field may suppress the observed thermal hysteresis at R-M phase transition.

In order to probe the substrate structural transformation effect on the magnetic behavior of the LSMO film, temperature, and field dependent magnetic measurements were performed. The initial magnetization curves from 0 Oe to 70kOe field were measured at different temperatures. M vs T curves for different temperatures are plotted in Figure 6(d). Two steps in the magnetization at ~180 K and ~285 K were observed found as an effect of R-M and M-T transition in BTO substrate, respectively. With the increase of magnetic field, the magnitude of the step vanishes above 10 kOe for R-M transition and 4 kOe for M-T transition, respectively. During the phase transition, the strain induced entropy changes in LSMO film due to the local anisotropy. As the local anisotropy is modified by the external magnetic field, the entropy is also changed. After a certain field, the modification of local magnetic anisotropy reaches its limit and the entropy as well. Hence, no further change is observed even as the magnetic field is increased. The entropy is much higher at low temperature and so the field required to completely vanish the entropy i.e. thermal hysteresis is also much higher.

The change of entropy at the R-M and M-T transitions as a function of magnetic field is shown in Figure 7. It is confirmed that the tunability of the entropy is much higher at the M-T transition which allows for magnetic control of caloric properties. The inset of Figure 7 shows the representative in-plane magnetic isotherms M(H) of LSMO film. Before measuring each M(H) isotherm, the sample was firstly heated up above T_C to avoid historic ferromagnetic domain configuration. The magnetic entropy change, $|\Delta S_M|$, at temperature T is obtained by using the Maxwell equation: [7, 18-21]

$$\Delta S_M(T, H) = S_M(T, H) - S_M(T, 0) = \int_0^H \left(\frac{\partial M}{\partial T} \right)_H dH \quad (3)$$

The values of $|\Delta S_M|$ are obtained by using Eq. 3 following standard procedures, i.e., the magnetization at selected fields $\mu_0 H$ is determined from the upper branches of the $M(H)$ loops ($H > 0$) measured at 5 K intervals away from the transition, 2 K intervals near the transition, and 1 K intervals across the transition. The highest value of magnetic entropy change ($\sim 5.87 \text{ J.kg}^{-1}.\text{K}^{-1}$ at $\mu_0 H = 50 \text{ kOe}$) was obtained near the M-T transition temperature as shown in Figure 7. There is a spike in entropy change near the M-T transition temperature. The values of ΔS are smaller than the peak value at the nearby temperature. These results are also independently confirmed by the Clausius - Clapeyron result as shown in the inset of Figure 7. The large value of $|\Delta S^{\max}_M| \times \delta T_{\text{FWHM}}$ ($\sim 140 \text{ J/kg}$) corresponds to the relative cooling power (RCP) of the sample. This large MCE arises from strain-mediated tuning of magnetic entropy originating from the first order structural phase transition of BTO. The substrate structural transformation corresponds to a reversal of magnetic anisotropy which reorients the magnetic easy axis along the film plane. In turn, this yields a noticeably large value of field dependent magnetic entropy change of 1.75 for 50 kOe, 1.03 for 30 kOe and 1.95 $\text{J.Kg}^{-1}.\text{K}^{-1}.\text{T}^{-1}$ for 10 kOe. These values are higher than previously reported values for other LSMO films on various substrates, e.g. 0.3 $\text{J.Kg}^{-1}.\text{K}^{-1}.\text{T}^{-1}$ for LSMO/LAO, 0.98 $\text{J.Kg}^{-1}.\text{K}^{-1}.\text{T}^{-1}$ for LSMO/LSAT, 0.89 $\text{J.Kg}^{-1}.\text{K}^{-1}.\text{T}^{-1}$ for LSMO/SRO and for bulk lanthanum manganite films. [7, 21-24]

4. Conclusion

In summary, we have studied the effect of magnetic field on the magnetocaloric properties of epitaxial 500 Å LSMO thin films grown on single crystal BTO. The large entropy change of 1.03-1.95 J.Kg⁻¹.K⁻¹.T⁻¹ was obtained at the monoclinic-tetragonal (M-T) transition at 283 K. Across the structural phase transitions, the thermal hysteresis is suppressed by the magnetic field and vanishes completely for the M-T and T-C transitions at high field. Such field-dependent magnetocaloric properties originate from the inhomogeneous strain in LSMO film induced by the different structural phase transitions in the BTO substrate. This inhomogeneous strain modifies the local magnetic anisotropy and thus entropy in the interfacial LSMO layers which can be manipulated by an external magnetic field, to different extents depending on the specific phase transition in question. The observed magnetic field-controlled magnetocaloric properties in LSMO/BTO film opens up the possibility of probing and manipulating magnetocaloric effects in similar materials, which would assist in the development of robust nanoscale magnetocaloric devices.

Acknowledgements

SKG thanks SERB-DST, Government of India for the financial support through award no. SB/OS/PDF-162/2016-17. We also acknowledge funding from the Leverhulme Trust grant RPG-2015-017, EPSRC grants (EP/L011700/1, EP/N004272/1 and EP/M000524/1). TM acknowledges funding from EU grant H2020-MSCA-IF-2016 745886 MuStMAM.

References

1. A. Kitanovski , U. Plaznic , U. Tomc , A. Poredoš , Int. J. Refrig. 57 , 288 (2015)
2. L. Mañosa , A. Planes , M. Acet , J. Mater. Chem. A 1, 4925 (2013)
3. X. Moya , S. Kar-Narayan , N.D. Mathur , Nat. Mater. 13, 439 (2014)

4. T. K. Nath, R. A. Rao, D.Lavric, C.B.Eom, L.Wu and F.Tsui, Appl. Phys. Lett. 74, 1615 (1999)
5. Y. Suzuki, H. Y. Hwang, S. W. Cheong and R. B. VanDover, Appl. Phys. Lett. 71, 140 (1997)
6. Y. Wu, Y. Suzuki, U.Rudiger, J. Yu, A.D. Kent, T.K. Nath and C.B. Eom, Appl. Phys. Lett. 75, 2295 (1999)
7. X. Moya, L. E. Hueso, F. Maccherozzi, A. I. Tovstolytkin, D. I. Podyalovskii, C. Ducati, L. C. Phillips, M. Ghidini, O. Hovorka, A. Berger, M. E. Vickers, E. Defay, S. S. Dhesi&N. D. Mathur, Nature Mater. 12, 52 (2013)
8. Y. Liu, S. G. E. teVelthuis, J. W. Freeland, H. Zhou, P. Steadman, P. Bencok, C. Leon, and J. Santamaria, APL Materials 4, 046105 (2016); S. Valencia, A. Crassous, L. Bocher, V. Garcia, X. Moya, R. O. Cherifi, C. Deranlot, K. Bouzehouane, S. Fusil, A. Zobelli , A. Gloter , N. D. Mathur , A. Gaupp , R. Abrudan, F. Radu , A. Barthélémy and M. Bibes, Nature Mater. 10, 753 (2011)
9. M. K. Lee, T. K. Nath, C. B. Eom, M. C. Smoak and F. Tsui, Appl. Phys. Lett.77,3547 (2000)
10. H. F. Tian, T. L. Qu, L. B. Luo, J. J. Yang, S. M. Guo, H. Y. Zhang, Y. G. Zhao and J. Q. Li, Appl. Phys. Lett.92,063507 (2008)
11. D. Dale, A. Fleet, J.D. Brock, Y. Suzuki, Appl. Phys. Lett.82,3725 (2003)
12. Y. P. Lee, S. Y. Park, Y. H. Hyun, J. B. Kim, V. G. Prokhorov, V. A. Komashko and V. L. Svetchnikov Phys. Rev. B 73, 224413 (2006)

13. A. Alberca, C. Munuera, J. Tornos, F. J. Mompean, N. Biskup, A. Ruiz, N. M. Nemes, A. de Andres, C. León, J. Santamaría, and M. García-Hernández; *Phys. Rev. B* 86, 144416 (2012)
14. F. D. Czeschka^{1, a)}, S. Geprägs¹, M. Opel¹, S. T. B. Goennenwein¹, and R. Gross; *Appl. Phys. Lett.* 95, 062508 (2009)
15. T. H. E. Lahtinen and S. Dijken; *Appl. Phys. Lett.* 102, 112406 (2013)
16. N. Mathur & P. Littlewood, *Phys. Today* **56**, 25 (2003)
17. A. J. Millis, T. Darling and A. Migliori, *J. Appl. Phys.* 83, 1588 (1998).
18. V. Suresh Kumar, Rami Chukka, Zuhuang Chen, Ping Yang and Lang Chen, *AIP Advances* 3, 052127 (2013)
19. Q Zhang, S Thota, F Guillou, P Padhan, V Hardy, A Wahland W Prellier, *J. Phys.: Condens. Matter* 23, 052201 (2011)
20. J. C. Debnath, J. H. Kim, Y. Heo, A. M. Strydom and S. X. Dou, *J. Appl. Phys.* 113, 063508 (2013)
21. S. K. Giri, Papri Dasgupta, A. Poddar, R. C. Sahoo, D. Paladhi, and T. K. Nath, *Appl. Phys. Lett.* 106, 023507 (2015)
22. D. T. Morelli, A. M. Mance, J. V. Mantese, and A. L. Micheli, *J. Appl. Phys.* 79(1), 373 (1996)
23. Q. Zhang, S. Thota, F. Guillou, P. Padhan, V. Hardy, A. Wahl and W. Prellier, *J. Phys. Condens. Matter* 23(5), 052201 (2011)
24. Donald T. Morelli, Andrew M. Mance, Joseph V. Mantese, and Adolph L. Micheli, *Journal of Applied Physics* 79, 373 (1996)

Figures

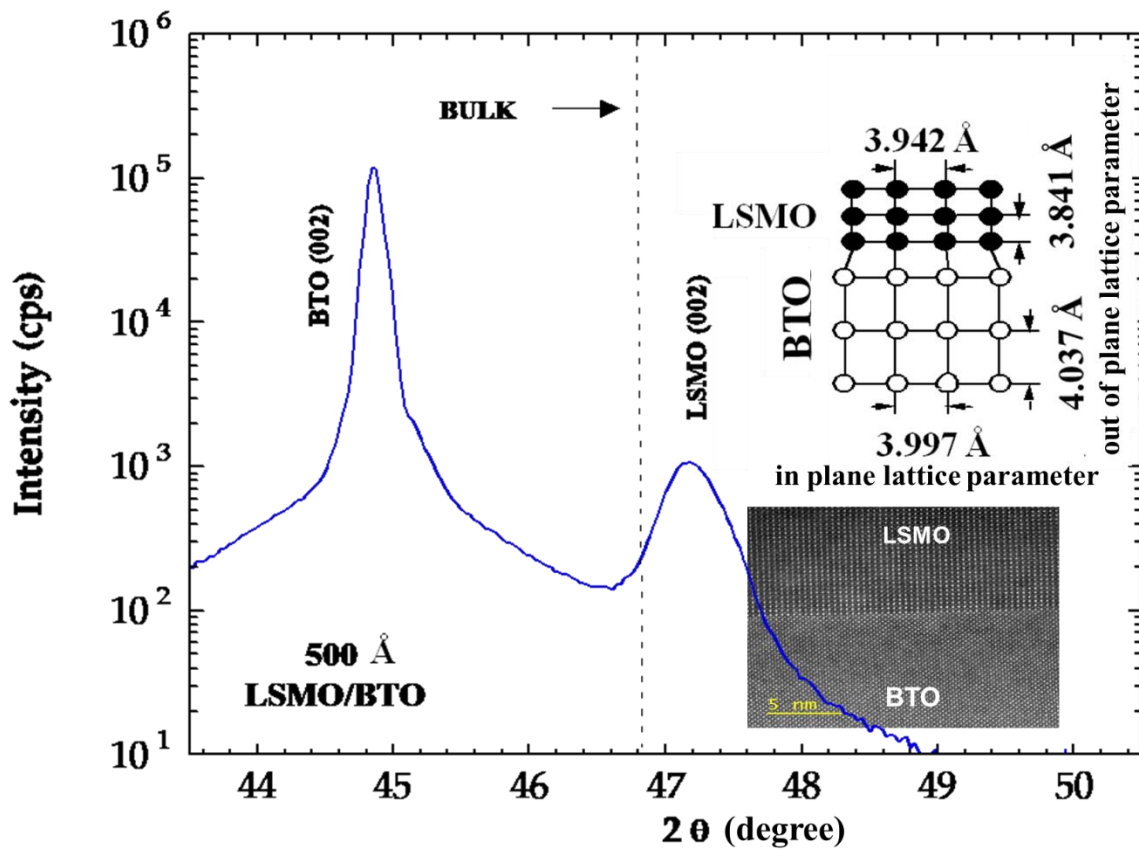


Figure 1: X-ray normal $\theta - 2\theta$ scans for 500 Å LSMO epitaxial films grown on (001) BTO substrates. The dotted line indicates bulk 2θ value of LSMO. Inset shows the schematic diagrams of cross-sectional view of the strained lattice. Inset shows the HRTEM image of LSMO/BTO epitaxial film.

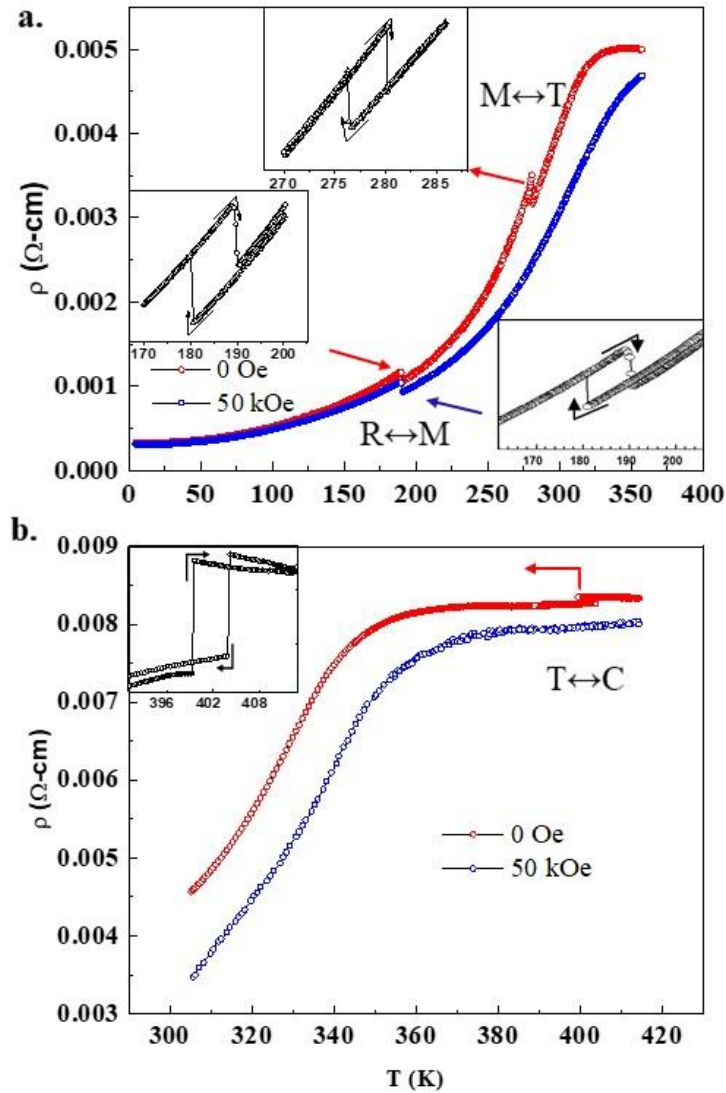


Figure 2. Resistivity versus temperature ($\rho(T)$) plots for a 500\AA LSMO/BTO epitaxial film without and with a 50000 Oe bias field over the temperature range of (a) 4.5 – 375 K and (b) 300 - 420 K. A sharp change in ρ for all three phase transitions of BTO was observed which vanishes at 50000 Oe bias field for the monoclinic to tetragonal (M-T) and tetragonal to cubic (T-C) transitions. The inset figures show the thermal hysteresis in the resistivity measurements as observed during the warming and cooling cycles. Upon application of a magnetic field, no thermal hysteresis was found for M-T and T-C transitions and the thermal hysteresis became smaller for the rhombohedral to monoclinic (R-M) transition.

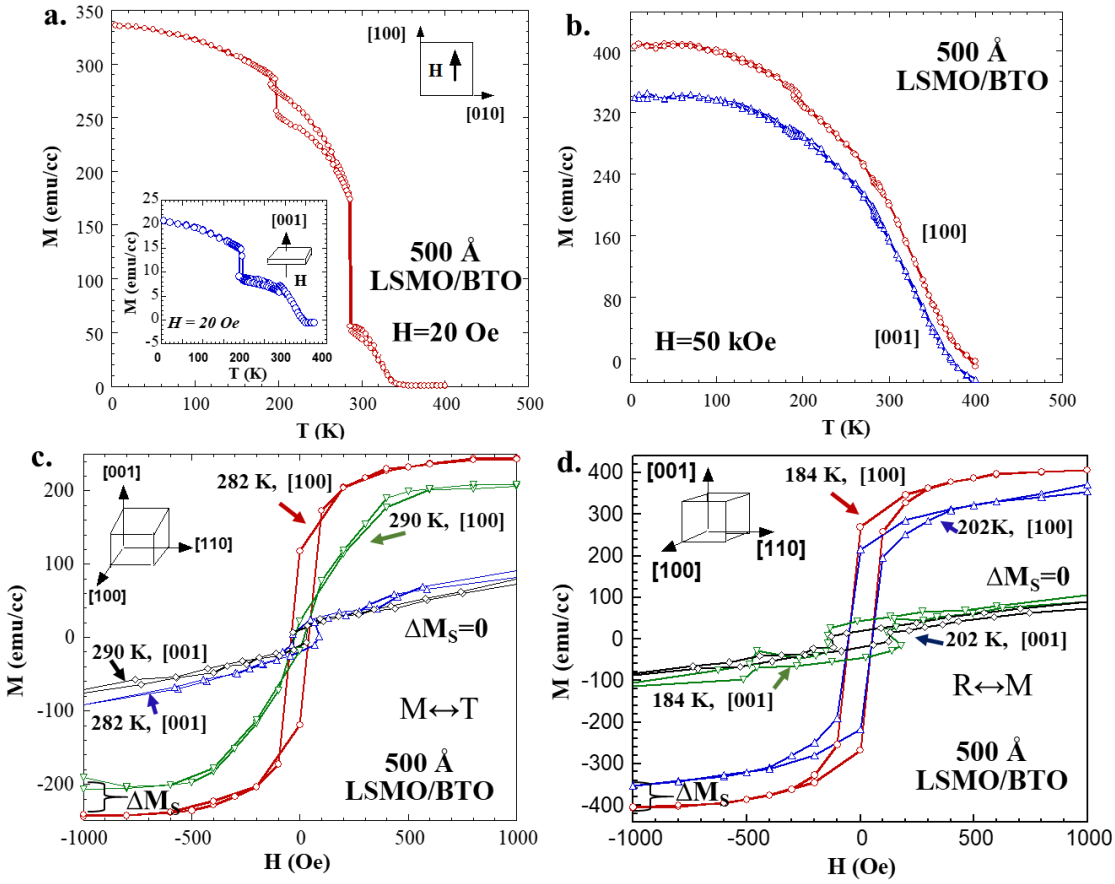


Figure 3. (a) $M(T)$ plot in both warming up and cooling down cycles at 20 Oe applied magnetic field along the in-plane [100] direction in 500 Å LSMO epitaxial films grown on [001] BTO. Inset shows the out-of-plane magnetization along [001] at 20 Oe field. (b) $M(T)$ plot along the in-plane [100] and out-of-plane [001] direction at 50000 Oe applied field for both warming cooling cycles. (c) Magnetic hysteresis loop at $T = 282$ and 290 K (below and above the monoclinic to tetragonal structural transformation (M-T) of the substrate) along the in-plane [100] and out-of-plane [001] directions. (d) Magnetic hysteresis loop at $T = 184$ and 202 K (below and above the orthorhombic to rhombohedral structural transformation of the substrate) along the in-plane [100] and out-of-plane [001] directions in 500 Å LSMO epitaxial films grown on [001] BTO.

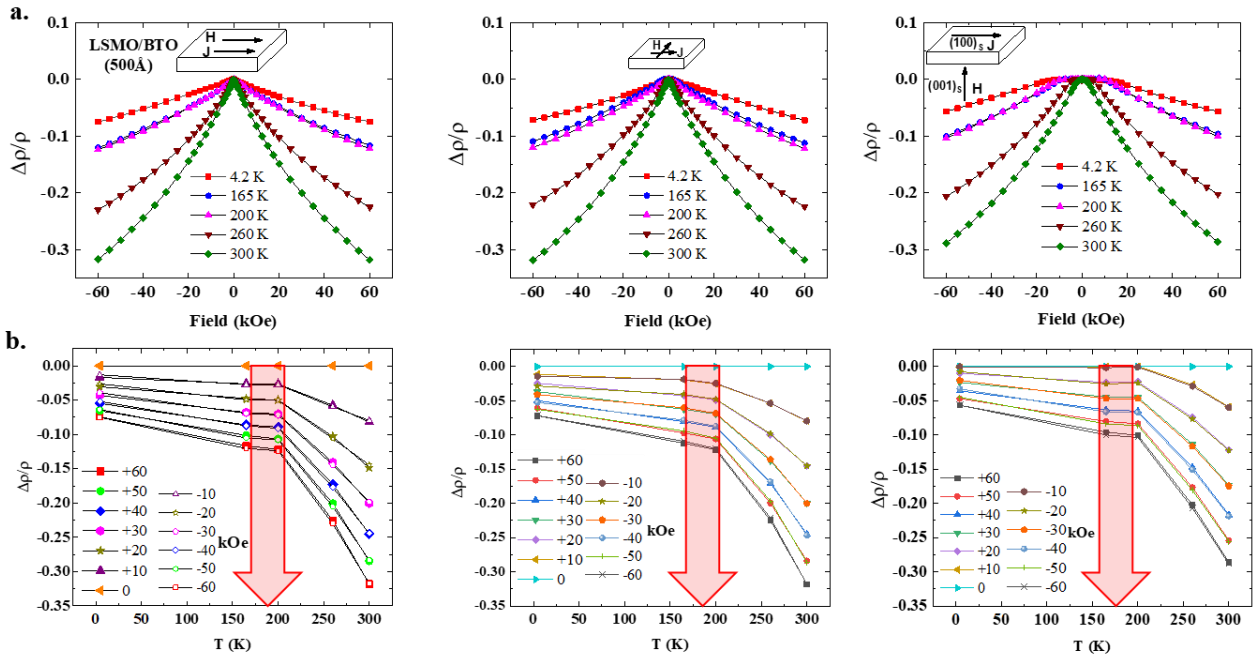


Figure 4. (a) MR curves for a 500 Å LSMO/BTO film at different temperature for three magnetic field configurations, magnetic field applied in the plane of the film and parallel to the current ($H \parallel J$), magnetic field applied in the plane of the film and perpendicular to the current ($H \perp J$) and magnetic field applied perpendicular to the current and the plane of the film ($H \odot J$). (b) Magnetic field (high) dependent resistivity change as a function of temperature.

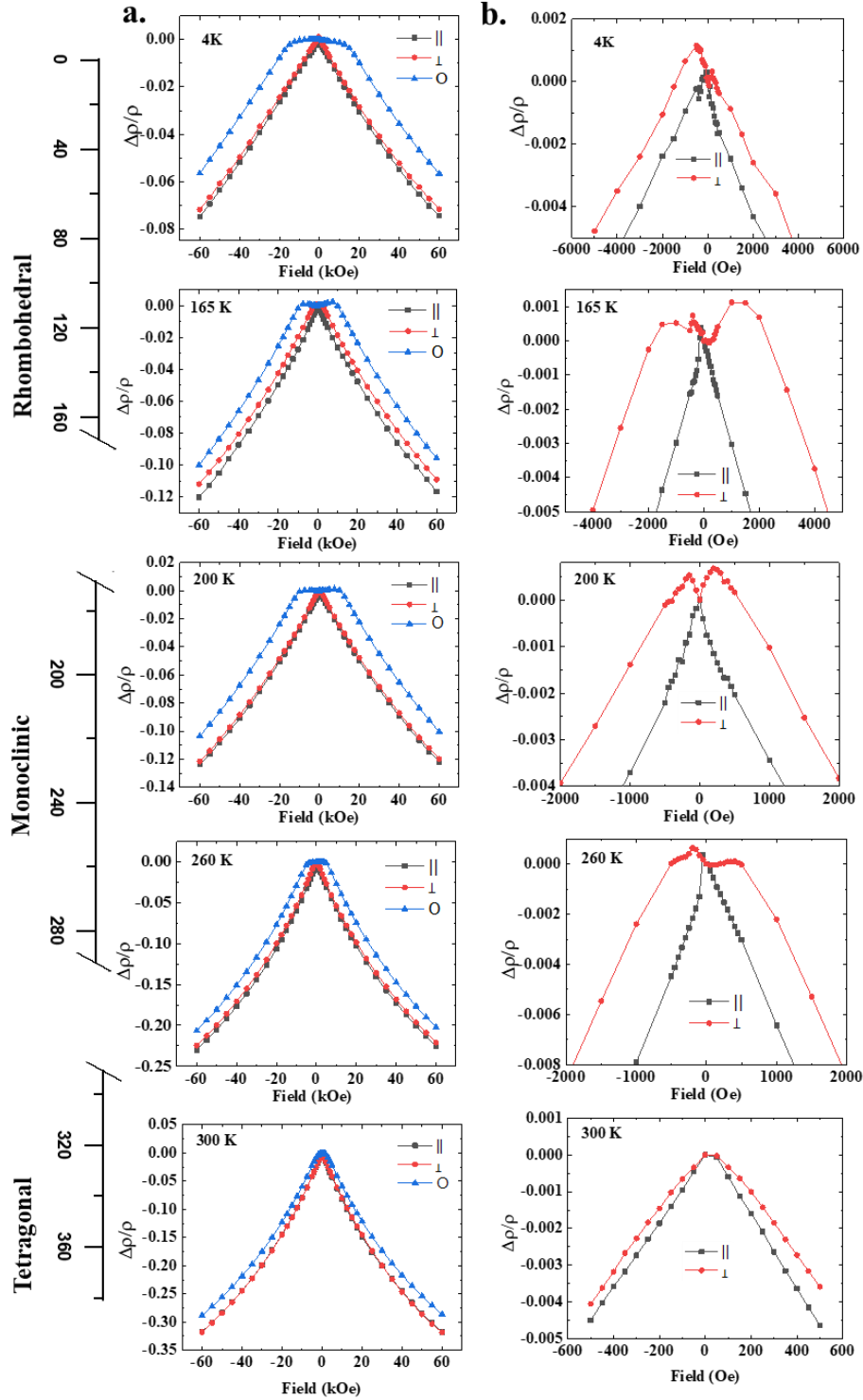


Figure 5. (a) MR curves for a 500 Å LSMO/BTO film at different temperature across different phase transitions in three different orientations. (b) Low field MR curve shows significant difference in the parallel and perpendicular directions.

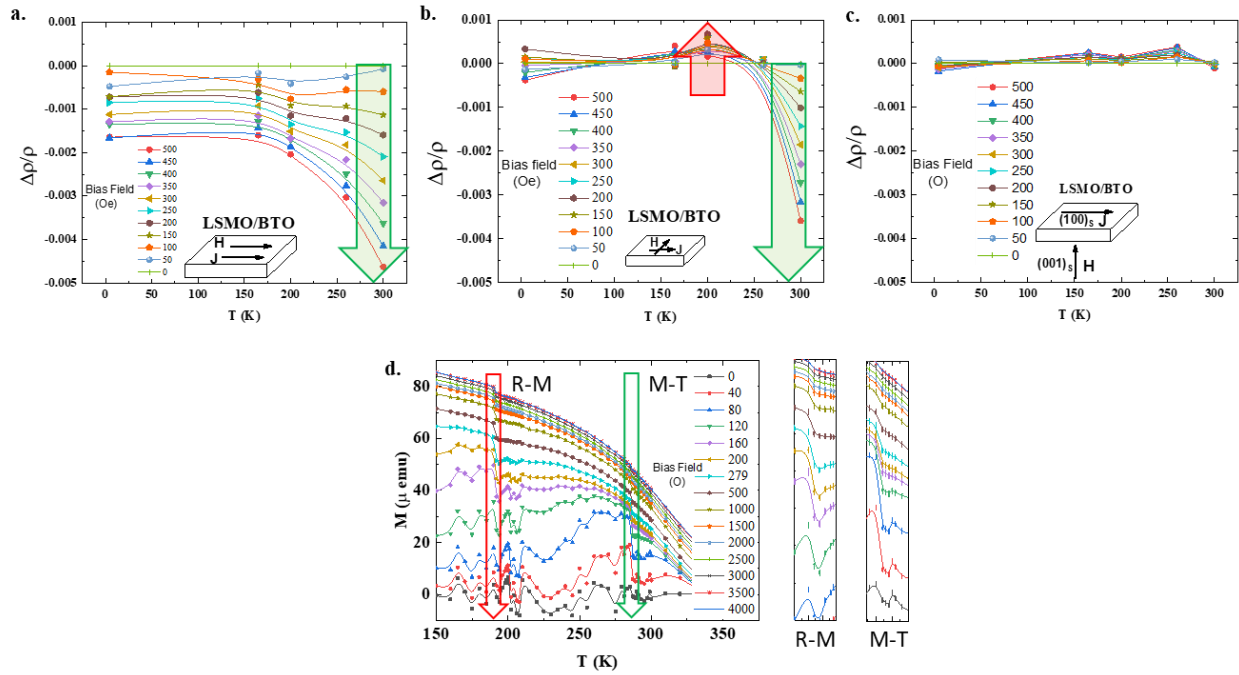


Figure 6. Magnetic field dependent resistivity measurements for 500 Å LSMO epitaxial films grown on [001] BTO plotted as function of temperature where the magnetic field (H) was applied in three different directions (a) parallel (\parallel), (b) perpendicular (\perp) and (c) out-of-plane (\odot) with respect to the current (J). (d) The temperature-dependent initial magnetization measurement for different bias fields is shown. A clear step is observed for the R-M and M-T transitions, which vanishes at higher fields.

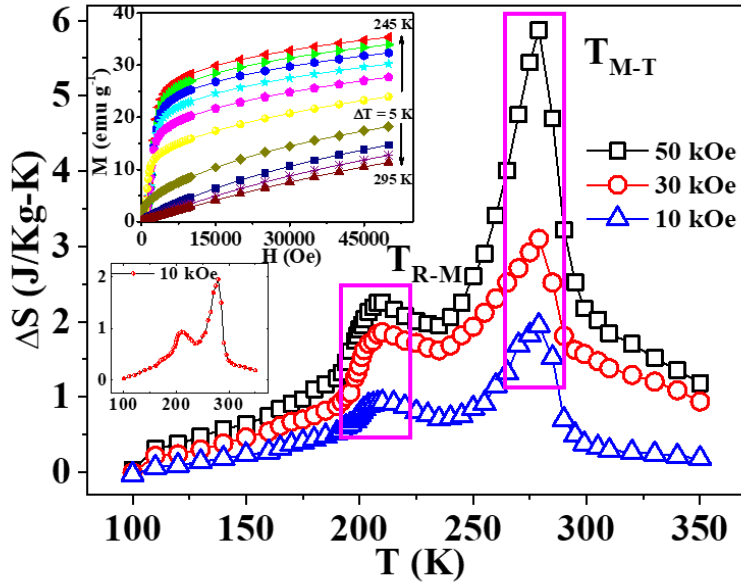


Figure 7. The ΔS vs. T curve of the sample at different magnetic fields. The values of isothermal entropy change at M-T transition is 1.75 (for 50 kOe), 1.03 (for 30 kOe) and 1.95 (for 10 kOe) $J.Kg^{-1}.K^{-1}.T^{-1}$. Inset shows the M-H curves at different temperatures and the ΔS vs. T curve calculated from the Clausius – Clapeyron equation.

Table 1: Biaxial Lattice distortion in the growth plane of (001) BTO substrate according to Eq. 2 at crystallographic structural transformation.

	R \rightarrow M	M \rightarrow T	T \rightarrow C
ϵ_{JT}	- 0.23 %	+ 0.25 %	+ 0.45 %